Available online at www.sciencedirect.com

ScienceDirect

Mendeleev Commun., 2024, **34**, 514–517

Mendeleev Communications

New pyridine dithiaazacrown ether derivatives: synthesis, structural characterization, *in silico* and *in vitro* biological studies

Van T. T. Tran,[a] Nhung T. Dao,[a] Thuyen T. Do,[a] Tam T. T. Pham,[b] Duan T. Le,[a] Victor N. Khrustalev,[c,d] Phuong T. T. Nguyen[e] and Anh T. Le*[a]

[a] *Faculty of Chemistry, University of Science, Vietnam National University, Hanoi, 100000 Hanoi, Vietnam. E-mail: huschemical.lab@gmail.com*
[b] *Thai Nguyen University of Medicine and Pharmacy, Thai Nguyen City, 250000 Thai Nguyen, Vietnam*
[c] *Peoples' Friendship University of Russia (RUDN University), 117198 Moscow, Russian Federation*
[d] *N. D. Zelinsky Institute of Organic Chemistry, Russian Academy of Sciences, 119991 Moscow, Russian Federation*
[e] *FPT University, Fschool Hoa Lac, Hanoi, Vietnam*

DOI: 10.1016/j.mencom.2024.06.014

New derivatives of dithiaazacrown ethers containing γ-arylpyridine subunits were prepared based on the Hantzsch synthesis. The obtained compounds showed potential activities toward Hep-G2 cancer cell line, in both *in silico* and *in vitro* studies. The compounds were also good ligands for complex chemistry with metal ions due to possessing up to four heteroatoms and relatively big size of the crown ring.

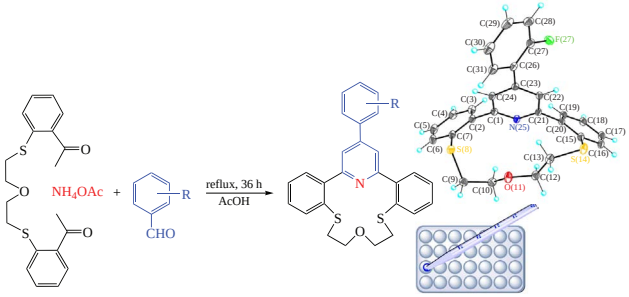

Keywords: dithiaazacrown ethers, arylpyridine subunit, Hantzsch synthesis, Hep-G2, crown ring.

Pyridine and piperidone derivatives find applications as pharmaceuticals.[1–4] Therefore, the synthesis of functionalized heterocycles containing γ-arylpyridine fragments is one of the primary goals for researchers.[5–8] The common approach is the Hantzsch pyridine synthesis which involves the assembling of three components, namely, β-keto ester or β-diketone, an aldehyde, and ammonia or a primary amine. Several pyridine-containing dibenzo macrocycles exhibited biological activities against various microbes with the MIC values ranging from ~3 to ~50 μg ml^{-1} (Figure 1).[9] The best overall performance was apparent for the compound with a disulfide bridge (X = SS).

Crown ethers have significant interests in chemistry and find applications in medicine, biotechnology, membranes, sensors, phase catalysts, energy, *etc*.[10–15] Up to date, the focus on synthetic methods as well as the chemical and biological properties of crown compounds is generally directed on the function of a crown chain. The introduction of biophore moieties into crown compounds is less studied. In our previous publications, several γ-arylpyridine-incorporating dibenzoaza-14-crown-4 ethers were synthesized, and their biological properties such as cytotoxic, antifungal, antibacterial and antioxidant activities were investigated[16–19] (compounds which expressed cytotoxic activities against the various human cancer cell lines are shown in Online Supplementary Materials, Figure S1). As a part of our ongoing research, this study presents the synthesis of new thiaazacrown ethers containing pyridine subunits based on the modification of Hantzsch reaction. Eight new compounds were prepared, and *in vitro* and *in silico* cytotoxicity evaluations were performed to investigate the structure–activity relationship.

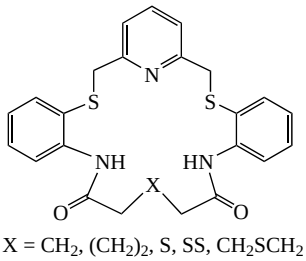

X = CH_2, $(CH_2)_2$, S, SS, CH_2SCH_2

Figure 1 Pyridine-containing macrocycles exhibiting toxicity to bacteria and fungi (*cf.* ref. 9).

Herein, the synthesis of dithaazacrown ether was performed in two steps. In the first step, precursor podand **1** was prepared according to the previous report.[19] In the second step, dibenzo-4,12-dithio-8-azacrownophanes **2a–h** were synthesized based on the modified multicomponent Hantzsch reaction between diketone **1**, aromatic aldehydes and ammonium acetate (Scheme 1).† Acetic acid was used as a solvent and catalyst,

† *Crystal data for* **2d**. The colorless prismatic crystal of **2d** ($C_{27}H_{22}FNOS_2$, M = 459.58) is monoclinic, space group $P2/n$, at T = 100 K, a = 15.3768(3), b = 7.9893(2) and c = 18.0456(4) Å, β = 97.6880(10)°, V = 2196.97(9) Å^3, Z = 4, d_{calc} = 1.390 g cm^{-3}, $F(000)$ = 960, μ = 0.272 mm^{-1}. A total of 53194 reflection intensities (8006 independent reflections, R_{int} = 0.0495) were measured using a Bruker D8 QUEST diffractometer equipped with a PHOTON-III area detector [λ (MoK_α)-radiation, graphite monochromator, ω and φ scanning mode] and corrected for absorption using the SADABS program (T_{min} = 0.864; T_{max} = 0.927). The structure was determined by direct methods and refined by a full-matrix least squares technique on F^2 with anisotropic displacement parameters for non-hydrogen atoms. The fluorine substituent is disordered over two sites with the occupancies of

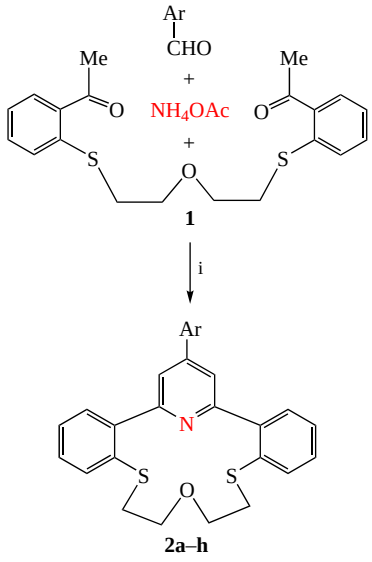

a Ar = 3-BrC_6H_4 **e** Ar = 2-$MeOC_6H_4$
b Ar = 2-ClC_6H_4 **f** Ar = 3-$O_2NC_6H_4$
c Ar = 3-ClC_6H_4 **g** Ar = 1,3-benzodioxol-5-yl
d Ar = 2-FC_6H_4 **h** Ar = 2-naphthyl

Scheme 1 *Reagents and conditions*: i, AcOH, reflux, 36 h.

refluxing the reactant mixture for 36 h afforded the target compounds. The highest yield (43%) was achieved for compound **2f** (see Table S1).

The experimental results showed that this modification of the Hantzsch reaction was affected by the nature of the starting aldehyde and diketone used. Figure S2 (see Online Supplementary Materials) shows the yield comparison between dithiacrown ether derivatives **2a**–**h** and their non-sulfur analogues with $O(CH_2)_2O(CH_2)_2O$ parts. The introduction of electron-withdrawing groups (such as F, Cl, Br, NO_2) at the *ortho*, *meta* and *para* positions of the aromatic aldehydes (RC_6H_4–CHO) provided a slightly higher yield of the corresponding pyridines compared to the case of compounds with an electron-donating substituent or without substituents. In addition, diketone with polyether chain $(OCH_2CH_2)_2O$ gave the corresponding pyridine derivatives with the overall yields higher than those for **2a**–**h**. Oxygen atom has an electronegativity of 3.44, whereas the sulfur atom has an electronegativity of 2.58. Consequently, the higher electron-attracting ability of oxygen facilitated the formation of methylene anion of ketone **1**, giving a better yield of the corresponding pyridine derivatives. Moreover, in the nucleophilic addition reaction of ketone **1** with aldehydes, oxygen atom with a smaller atomic radius than that of sulfur atom leads to the lesser steric hindrance of polyether chain *vs*. polythioether chain. The structure of newly synthesized products was confirmed by spectral data analysis.

Compound **2d** was additionally characterized by single-crystal X-ray diffraction study (Figure 2).† The calculations were executed using the SHELXTL program.[20–22] Overall, the molecule **2d** possesses the idealized C_s (*m*) intrinsic symmetry. However, in the crystal, the geometry of **2d** is significantly

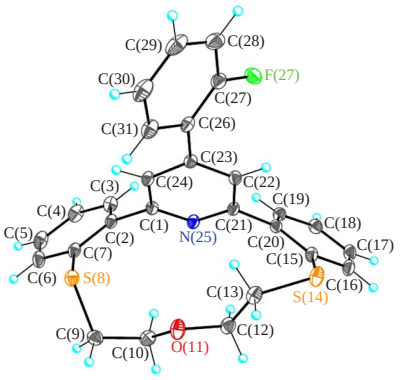

Figure 2 Molecular structure of **2d** (50% ellipsoids). The alternative position of the disordered fluorine substituent with the minor occupancy is not shown.

distinguished from the idealized one due to the presence of the intermolecular S···S interactions as well as the crystal packing effects. Molecule **2d** consists of a fused tetracyclic system containing the aza-dithia-14-crown-4-ether macrocycle, pyridine and two benzene rings. The aza-dithia-14-crown-4-ether ring adopts a bowl conformation. The configuration of the C(7)–S(8)–C(9)–C(10)–O(11)–C(12)–C(13)–S(14)–C(15) aza-dithia-ether chain is g^+–g^+–*t*–*t*–*t*–g^+ (*t* = *trans*, 180°; *g* = *gauche*, ±60°). The dihedral angles between the planes of the central pyridine and two benzene rings fused to the aza-dithia-14-crown-4-ether moiety are 64.53(4) and 59.84(4)°. The fluorophenyl substituent is twisted relative to the parent pyridine ring by 43.37(4)°.

In the crystal, molecules **2d** form the dimers by the intermolecular S···S [3.4378(6) Å] interactions (Figure 3). The dimers occupy a special position on the two-fold axis and are arranged at van der Waals distances (see Online Supplementary Materials, Figures S3, S4). In addition, the size of the internal cavity of dithiacrown ether derivatives was determined as the double average distance between the cyclic n-electron- donor heteroatoms and the centroid of the $N_{25}S_8S_{14}O_{11}$ ring (Figure S5).[23,24] This value for compound **2d** is 5.297 Å. In comparison with other azacrown ether derivatives, dithiacrown ether derivatives have bigger internal cavity.[25] This is attributed to the larger atomic radius of sulfur atoms present in these molecules. Obtained compounds are good source for other chemical transformations as well as host–guest chemistry.[26]

Cytotoxicity activities of synthesized compounds **2a**–**f** against human tumor cell lines, including Hep-G2 (*human hepatocellular carcinoma*), MCF7 (*human breast adenocarcinoma*), Hela (*HeLa cervical cancer cells*), A594 (*Human lung carcinoma*), and Vero cell were evaluated using Sulforhodamine B (SRB) method as described by Likhiwitayawuid and Skehan.[27,28] Ellipticine served as the control drug. IC_{50} values were defined as the concentration that reduced the viable cells by 50% compared to the untreated

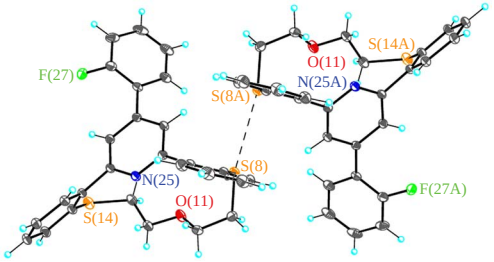

Figure 3 Dimer of the molecules of **2d** connected *via* the intermolecular S···S interaction. The alternative positions of the disordered fluorine substituents with the minor occupancies are not shown.

0.9 : 0.1. The hydrogen atoms were placed in calculated positions and refined within riding model with fixed isotropic displacement parameters [U_{iso}(H) = 1.2U_{eq}(C)]. The final divergence factors were R_1 = 0.0418 for 6372 independent reflections with $I > 2\sigma(I)$ and wR_2 = 0.1108 for all independent reflections, S = 1.025. All calculations were carried out using the SHELXTL program.

CCDC 2298591 contains supplementary crystallographic data for this paper. These data can be obtained free of charge from the Cambridge Crystallographic Data Centre *via* http://www.ccdc.cam.ac.uk.

control cells. All experiments were conducted in triplicate and all data are expressed as the mean ± standard deviation. Among six studied compounds, only fluorinated compound **2d** expressed activity against the Hep-G2 cell line with an IC_{50} of 17.76 μg ml^{-1} (38 μM) (see Online Supplementary Materials). To explore the interaction of inhibitors and enzyme's active sites, molecular docking of the most potent inhibitor **2d** was studied using Autodock vina software.[29] The macromolecule structure for the EGFR tyrosine kinase domain inhibitor Erlotinib (PDB: 1M17) was obtained from the protein data bank (https://www.rcsb.org/structure/1M17). After download, EGFR tyrosine kinase was deprived of water molecule, ligand and hetatoms, polar hydrogens and Kollman charges were added, then Erlotinib was docked into the binding sites of protein structure to perform the verification process. Erlotinib is an US FDA approved drug for the treatment of lung cancer, which inhibits the EGFR kinase by binding to the ATP binding site and by forming a hydrogen bond with the backbone NH of the hinge region Met769 amino acid.[30,31] Finally, our compounds were docked to the same binding site of EGFR tyrosine kinase as Erlotinib. The calculation has been carried out using an Intel (R) Core (TM) i3-10400 CPU @ 2.90 GHz workstation. Visualization of ligand–receptor interactions was performed using Discovery Studio 2021. Compound **2d** shows interaction with 6 amino acids of EGFR tyrosine kinase by forming Carbon hydrogen, Halogen (Fluorine), π–sigma, π−sulfur, π−π stacking and π−alkyl bonds (Table 1 and Figures 4, 5). The main parts of molecule **2d** participating in these interactions came from the phenyl and pyridine moieties. Polythioether chain contributes only one interaction with Arg 817 amino acid.

The calculation revealed that compound **2d** was highly potent inhibitor of Hep-G2 due to its binding energy of –10.2 kcal mol^{-1}, which is lower than that of Erlotinib (–7.2 kcal mol^{-1}). According to *in vitro* study, activity of Ellipticine was 38-fold higher over **2d**. In this case, the most active of Erlotinib is due to the large number of interactions with receptor and the lower of molecular energy (212.36 kJ mol^{-1}) which contributes to stabilizing its complex with receptor. In addition, 13 properties of compound **2d** as well as its drug-like ranges (upper and lower limits) were predicted using the ADMET tool. Figure 6 shows the computed results in which the parameters of compound **2d** fall within the optimal range, except their lipophilicity (characterized by log*P* and log*D* values) and their number of atoms in the largest ring (MaxRing). The number of rigid bonds (nRig) is slightly higher than upper limit. This calculation demonstrated relative accordance with the *in vitro* bioassay of **2d**.

In conclusion, eight γ-arylpyridine-incorporating dibenzoaza-14-dithiacrown-4 derivatives were prepared in reasonable yields, and their bioactivities were estimated in both *in silico* and *in vitro* experiments. The representative **2d** bearing 3-fluorophenyl

Table 1 The binding affinity and RMSD values of compounds **2d** and Erlotinib.

Compound	Binding energy /kcal mol^{-1}	Distance from best mode (RMSD)	2D interaction with amino acids	Molecular energy /kJ mol^{-1}
2d	–10.2	0.000	Val702, Lys721, Asp831, Phe699, Arg817, Cys751	571.789
Erlotinib	–7.2	0.000	Met769, Leu694, Leu820, Ala719, Val702, Gly772, Gln767, Lys721, Met742, Thr830, Leu764	212.36

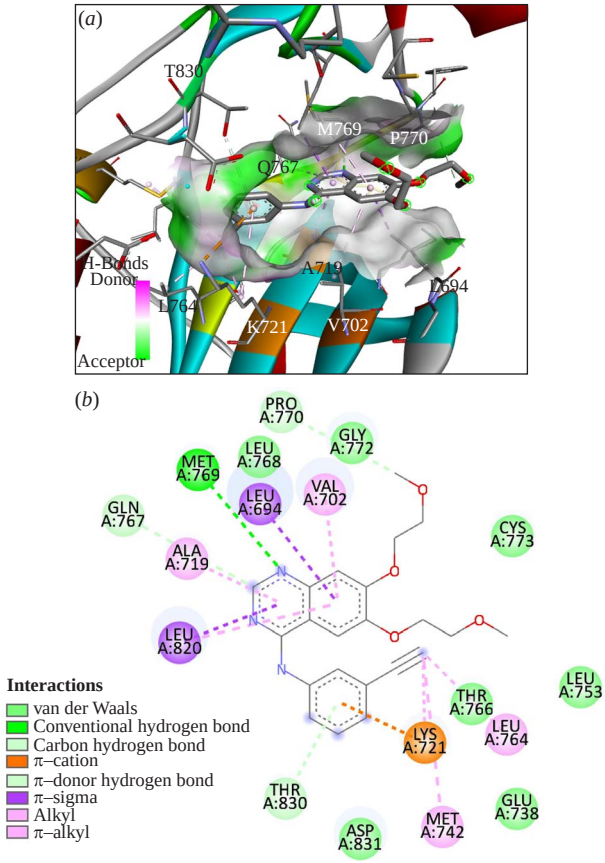

Figure 4 The interactions of Erlotinib docked into the macromolecule 1M17: (*a*) 3D and (*b*) 2D.

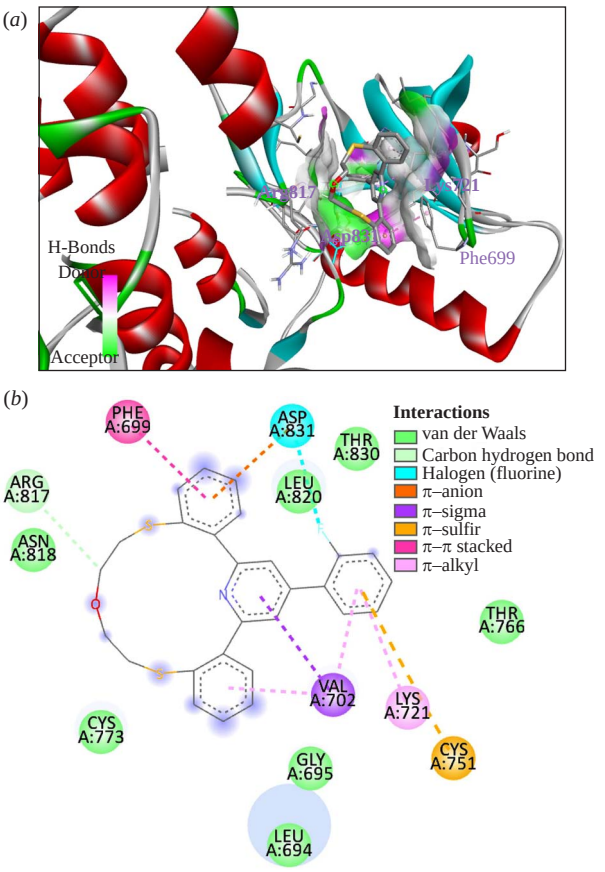

Figure 5 The interactions of compound **2d** docked into the macromolecule 1M17: (*a*) 3D and (*b*) 2D.

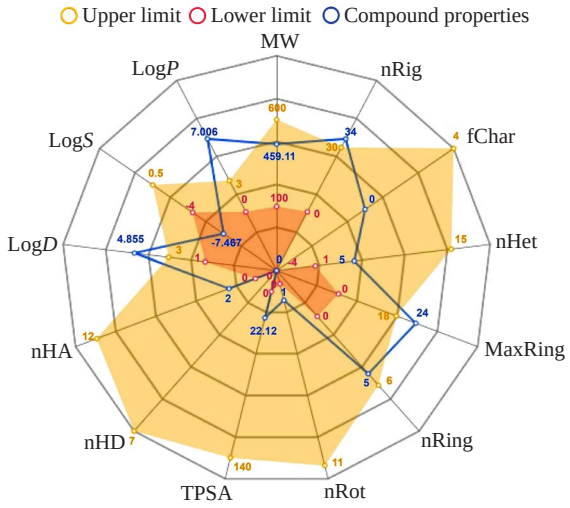

Figure 6 Drug likeness of compound **2d**.

substituent expressed activity against Hep-G2 cell line with IC_{50} of 38 μM and did not show toxic toward Vero cell lines. Molecular docking study indicated that a flourine atom and aromatic parts of **2d** contribute five interactions with various amino acids of EGFR tyrosine kinase. This implies that the modification of substituents of starting aldehydes significantly influences both the yield of reaction and the bioactivities of the final products.

This research has been done under the research project QG.22.13 of Vietnam National University, Hanoi and has been supported by the RUDN University Strategic Academy Leadership Program.

Online Supplementary Materials

Supplementary data associated with this article can be found in the online version at doi: 10.1016/j.mencom.2024.06.014.

References

1 K.-Y. Jun, H. Kwon, S.-E. Park, E. Lee, R. Karki, P. Thapa, J.-H. Lee, E.-S. Lee and Y. Kwon, *Eur. J. Med. Chem*., 2014, **80**, 428.
2 P. Thapa, R. Karki, M. Yun, T. M. Kadayat, E. Lee, H. B. Kwon, Y. Na, W.-J. Cho, N. D. Kim, B.-S. Jeong, Y. Kwon and E.-S. Lee, *Eur. J. Med. Chem*., 2012, **52**, 126.
3 R. Karki, P. Thapa, H. Y. Yoo, T. M. Kadayat, P.-H. Park, Y. Na, E. Lee, K.-H. Jeon, W.-J. Cho, H. Choi, Y. Kwon and E.-S. Lee, *Eur. J. Med. Chem*., 2012, **49**, 219.
4 R. Karki, P. Thapa, M.-J. Kang, T.-C. Jeong, J.-M. Nam, H. L. Kim, Y. Na, W.-J. Cho, Y. Kwon and E.-S. Lee, *Bioorg. Med. Chem*., 2010, **18**, 3066.
5 X. Qi, H. Xiang, Q. He and C. Yang, *Org. Lett*., 2014, **16**, 4186.
6 L.-Y. Xi, R.-Y. Zhang, S. Liang, S.-Y. Chen and X.-Q. Yu, *Org. Lett*., 2014, **16**, 5269.
7 H. Wei, Y. Li, K. Xiao, B. Cheng, H. Wang, L. Hu and H. Zhai, *Org. Lett*., 2015, **17**, 5974.
8 Y. Wei and N. Yoshikai, *J. Am. Chem. Soc*., 2013, **135**, 3756.
9 Ö. Zaim, N. M. Aghatabay, M. U. Gürbüz, Ç. Baydar and B. Dülger, *J. Inclusion Phenom. Macrocyclic Chem*., 2014, **78**, 151.
10 M. Ganjali, P. Norouzi, M. Rezapour, F. Faridbod and M. Pourjavid, *Sensors*, 2006, **6**, 1018.
11 L. He, T. Zhan, C. Zhu, T. Yan and J. Liu, *Chem. – Eur. J*., 2023, **29**, 202300044.
12 C. Yoo, H. M. Dodge and A. J. M. Miller, *Chem. Commun*., 2019, **55**, 5047.
13 U. Faiz, A. K Taskin, I. Jawaria, A. Saleha, F. A. K. Muhammad, R. K Muhammad, U. Sami, F. R. Muhammad, M. Muhammad, K. Kotwica-Mojzych and M. Mariusz, *Appl. Sci*., 2022, **12**, 1102.
14 T. Yokoyama and M. Mizuguchi, *J. Med. Chem*., 2019, **62**, 2076.
15 Y. Zeng, H. Pei, Z. Wang, F. Yan, J. Li, Z. Cui and B. He, *ACS Omega*, 2018, **3**, 554.
16 A. T. Le, H. H. Truong, P. T. T. Nguyen, H. T. Pham, V. E. Kotsuba, A. T. Soldatenkov, V. N. Khrustalev and A. T. Wodajo, *Macroheterocycles/ Makrogeterotsikly*, 2014, **7**, 386.
17 A. T. Le, H. H. Truong, P. T. T. Nguyen, N. T. Dao, H. T. To, H. T. Pham and A. T. Soldatenkov, *Mendeleev Commun.*, 2015, **25**, 224.
18 A. T. Le, H. H. Truong, P. T. T. Nguyen, T. T. V. Tran, N. T. Dao and A. T. Soldatenkov, *Vietnam J. Chem*., 2015, **53(4e1)**, 141.
19 T. T. P. Thi, T. T. Do, D. T. Nguyen, V. B. Luu, E. I. Polyakova, T. V. T. Thi and A. T. Le, *Chem. Heterocycl. Compd*., 2020, **56**, 1234.
20 L. Krause, R. Herbst-Irmer, G. M. Sheldrick and D. Stalke, *J. Appl. Crystallogr*., 2015, **48**, 3.
21 G. M. Sheldrick, *Acta Crystallogr*., 2015, **A71**, 3.
22 G. M. Sheldrick, *Acta Crystallogr*., 2015, **C71**, 3.
23 A. N. Levov, L. T. An', A. I. Komarova, V. M. Strokina, A. T. Soldatenkov and V. N. Khrustalev, *Russ. J. Org. Chem*., 2008, **44**, 456 (*Zh. Org. Khim*., 2008, **44**, 457).
24 D. T. Nguyen, H. H. Truong, N. T. Dao, V. T. T. Tran, O. S. Gorchakova and A. T. Le, *Mendeleev Commun*., 2023, **33**, 708.
25 N. T. Dao, T. T. Do, T. T. T. Pham, V. T. T. Tran, V. N. Khrustalev and A. T. Le, *Mendeleev Commun*., 2023, **33**, 711.
26 A. N. Levov, A. I. Komarova, A. T. Soldatenkov, G. V. Avramenko, S. A. Soldatova and V. N. Khrustalev, *Russ. J. Org. Chem*., 2008, **44**, 1665 (*Zh. Org. Khim*., 2008, **44**, 1688).
27 P. Skehan, R. Storeng, D. Scudiero, A. Monks, J. McMahon, D. Vistica, J. T. Warren, H. Bokesch, S. Kenney and M. R. Boyd, *J. Natl. Cancer Inst*., 1990, **82**, 1107.
28 K. Likhitayawuid and C. K. Angerhofer, *J. Nat. Prod*., 1993, **56**, 30.
29 G. M. Morris, R. Huey, W. Lindstrom, M. F. Sanner, R. K. Belew, D. S. Goodsell and A. J. Olson, *J. Comput. Chem*., 2009, **30**, 2785.
30 M. H. Cohen, J. R. Johnson, Y.-F. Chen, R. Sridhara and R. Pazdur, *Oncologist*, 2005, **10**, 461.
31 J. Stamos, M. X. Sliwkowski and C. Eigenbrot, *J. Biol. Chem*., 2022, **277**, 46265.

Received: 15th December 2023; Com. 23/7345